Springer

Journal of Mechanical Science and Technology 23 (2009) 814~822

Journal of
Mechanical
Science and
Technology

www.springerlink.com/content/1738-494x
DOI 10.1007/s12206-009-0206-x

Electroosmotically enhanced microchannel heat sinks †

Afzal Husain and Kwang-Yong Kim*

Department of Mechanical Engineering, Inha University, Incheon, 402-751, Republic of Korea

(Manuscript Received June 30, 2008; Revised November 19, 2008; Accepted February 2, 2009)

Abstract

The present study investigates the microchannel heat sink for pure electroosmotic, pressure-driven, and mixed (electroosmotic and pressure-driven) flows. A three-dimensional numerical analysis is performed for electroosmotic and mixed flows. Electroosmotic flow (EOF) induced in an ionic solution in the presence of surface charge and electric field is investigated with hydrodynamic pressure-driven flow (PDF) to enhance heat removal through the microchannel heat sink. In a pressure-driven microchannel heat sink, the application of an external electric field increases the flow rate that consequently reduces the thermal resistance. The effects of ionic concentration represented by the zeta potential and Debye thickness are studied with the various steps of externally applied electric potential. A higher value of zeta potential leads to higher flow rate and lower thermal resistance, which consequently reduce the temperature of the microprocessor chip and load of the micropump used to supply coolant to the microchannels.

Keywords: Electroosmotic flow; Microchannel heat sink; Numerical simulation; Thermal resistance

1. Introduction

The rapid increase in the ultra large-scale integration (ULSI) circuit density and challenges in multichip integration motivated the designers to opt for non-traditional cooling techniques for microprocessors. Liquid cooling is more effective in ULSI and can be used to remove localized heat flux as well. Many studies have been conducted using various techniques such as experimental, analytical, and numerical after Tuckerman and Pease [1] conducted experiments on a silicon-based microchannel heat sink for electronic cooling. A state-of-the-art single-phase forced convection was reviewed by Yener et al. [2]. They concluded that liquid flow in microchannels is in a continuum regime, but classical correlations used for conventional-sized channels indicate a significant departure from the experimental investigations of microchannels. The three-dimensional numerical analysis for fluid flow and heat transfer was performed for a rectangular microchannel heat sink for constant and variable fluid properties [3-5]. The researchers found numerical predictions within the experimental uncertainties. The above studies show that three-dimensional numerical analyses can be used to qualitatively characterize the microchannel heat sink for pressure-driven flow (PDF).

Conventional micropumps posed limitations in terms of efficiency and reliability, which opened the doors for alternative methods to drive the fluid through microchannels. Joshi and Wei [6] performed an exhaustive survey of electronic thermal management based on micro- and meso-scale compact heat exchangers. They identified the need for further research in the area of micropumps, which appears to be insufficient to provide potential pumping power for electronic cooling. The problem of driving the fluid through microchannels becomes more significant when the dimensions of the device channel reach close to the order of the thickness of the electric dou-

† This paper was recommended for publication in revised form by Associate Editor Do Hyung Lee

* Corresponding author. Tel.: +82 32 872 3096, Fax.: +82 32 868 1716
E-mail address: kykim@inha.ac.kr

ble layer (EDL). The growing requirement of pumping power in various applications, such as chemical analysis and in the medicine industry, and the eagerness for the removal of higher flux from microcooling devices used in various systems such as micro refrigerators, avionics, robotics, electronic industry, and others have encouraged the usage of electroosmotic pumping for these applications. Laser and Santiago [7] carried out a survey on micropumps and found that electroosmotic micropumps provide favorable flow rates and pressure heads, emerging as a viable option for a number of applications including integrated circuit thermal management, although the working fluid should be electrically inert to avoid accidental leakage [6].

Electroosmotic flow (EOF) is the bulk motion of the fluid under the influence of an externally applied electric field. Mala et al. [8] carried out an investigation for the effects of EDL on a solid liquid interface for liquid flows through a microchannel between two parallel plates both experimentally and theoretically. They observed that the friction coefficient increased in low ionic concentration and high zeta potential. However, in microchannels with a hydraulic diameter greater than a few hundred micrometers, the EDL effects were negligible. Yang et al. [9] demonstrated the electrokinetic effects in a pressure-driven rectangular microchannel and found that the EDL field and induced electrokinetic potential act against the liquid flow, resulting in the reduction in Nusselt number and increase in friction coefficient. Arulanandam and Li [10] investigated EOF with the help of two-dimensional Poisson-Boltzmann and two-dimensional momentum equations. They characterized the flow on the basis of cross-section ion concentration and zeta potential in the absence of significant joule heating. Jiang et al. [11] proposed and characterized an ultra compact closed-loop two-phase microcooling system. They demonstrated the design, fabrication, and performance of this heat exchanger and electroosmotic pumping application in a very large-scale integration (VLSI) chip.

Patankar and Hu [12] proposed a three-dimensional numerical scheme based on Debye-Huckel approximations to simulate electrokinetic flow. Morini et al. [13] numerically investigated the EOFs in the microchannel heat sinks of rectangular and trapezoidal cross-sections. They studied the effects of dimensionless electroosmotic diameter κDh and geometry aspect ratio on the cross sectional Nusselt number and suggested the application of electroosmotically-driven microchannel heat sink for a low heat flux removal rate. Dutta et al. [14] investigated thermal characteristics in a two-dimensional channel for pure electroosmotic and mixed (electroosmotic and pressure driven) flows. They found that the heat transfer coefficient for pure EOF is higher than the mixed flow and pure PDF. Jain and Jensen [15] investigated the effects of electrokinetics on microchannel fluid flow and heat transfer using a linearized Poisson-Boltzmann equation. They found that the presence of EDL reduces the fluid velocity in the EDL regime, but the effect of electrokinetics on the heat transfer is quite small. Tang et al. [16] highlighted the significance of joule heating in EOF. They found that a higher concentration leads to higher joule heating effects, which accelerates the sample transport and distortion of the velocity profile and the band broadening and reduction of the peak.

The bulk motion induced by an externally applied electric field has been investigated in pure electroosmotic and in mixed electroosmotic and PDF. The ion concentration and applied electric field that govern the body force contributing to the Navier-Stokes equation have been studied for the application to microchannel heat sink. The feasibility of pure electroosmotic and mixed flow (EOF+PDF) microchannel heat sink in electronic cooling applications has been studied in light of the ionic concentration and applied electric field.

2. Geometric and numerical model

The schematic of a rectangular microchannel heat sink investigated in the present study is shown in Fig. 1. The overall dimensions of the heat sink are 10mm×10mm×0.5mm, with a moderate aspect ratio (W_c/H_c) of 0.175, fin width (W_w) of 30 μm, and channel depth (H_c) of 400 μm. Due to the symmetry of the microchannels in the lateral direction, half of the single microchannel has been taken as the computational domain as shown in Fig. 1. In most microfluidic devices, the walls of the microchannels are made of dielectric materials and surface charge. If an ionic fluid comes in contact with the charged surface, the counter ions present in the fluid move towards the surface and form an electric double layer as shown in Fig. 2. Outside the EDL, both coions and counterions have the same concentration. When an external electric potential is applied to the microchannel, the dif-

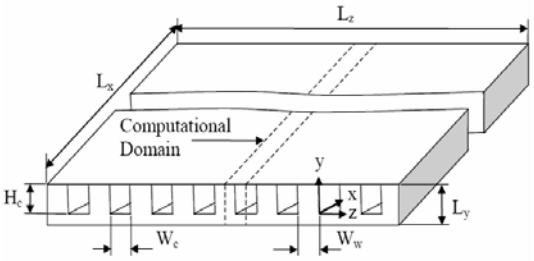

Fig. 1. Schematic of a microchannel heat sink.

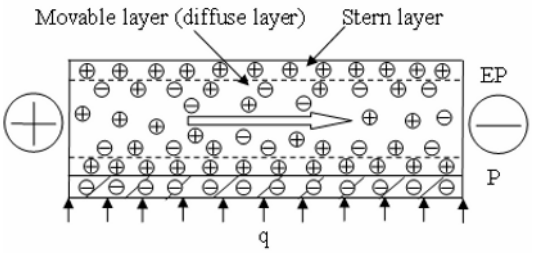

Fig. 2. Schematic diagram of the electric double layer in a microchannel.

fuse layer of the EDL is activated, and the movements of ions take place. In the steady state, the balance between the electroosmotic force on the ions and viscous drag force on the fluid result in a plug-like velocity profile. Mathematically, this electroosmotic force is treated as a body force in the Navier-Stokes formulation. Thus, the EOF is governed by continuity and the Navier-Stokes equations with a body force term due to the electric field:

$$\nabla \cdot \mathbf{u} = 0 \tag{1}$$

$$\rho_f (\mathbf{u} \cdot \nabla)\mathbf{u} = -\nabla p + \mu_f \nabla^2 \mathbf{u} + \rho_e \mathbf{E} \tag{2}$$

where electric field is related to the electric potential by

$$\mathbf{E} = -\nabla \Phi \tag{3}$$

The electric potential is governed by the Poisson equation as follows:

$$\nabla^2 \Phi = -\rho_e / \varepsilon \tag{4}$$

As the Debye thickness is small in comparison with the microchannel width/height, and the charge at the wall is also small, the distribution of the charge in the diffuse layer is mainly governed by the zeta potential at the wall. The external electric field has very little effect on the charge distribution within the diffuse layer of the EDL; therefore, the charge distribution near the walls can be treated independent of the externally applied electric field, and the equations of the electric field and flow field can be decoupled as suggested by Patankar and Hu [12] as follows:

$$\Phi = \phi + \psi \tag{5}$$

Furthermore,

$$\nabla^2 \phi = 0 \tag{6}$$

and

$$\nabla^2 \psi = -\rho_e / \varepsilon \tag{7}$$

The induced electric field is directed normally to the wall; thus, it does not contribute to the main flow. The effective electric field that exerts a force on the charged species which induces electroosmotic flow can be approximated in terms of the external electric potential as:

$$\mathbf{E} = -\nabla \phi \tag{8}$$

The EDL can be modeled as a diffuse layer using charge distribution as proposed in the Gouy-Chapman theory [17]; thus, the ion distribution satisfies the Boltzmann statistics. Therefore, Eq. (7) can be written in the form of a linearized Poisson-Boltzmann equation as follows:

$$\nabla^2 \psi = \kappa^2 \psi \tag{9}$$

where κ^{-1} is the Debye length, representing the Debye layer thickness. By substituting Eq. (9) for Eq. (7), the electrical charge density can be written as follows:

$$\rho_e = -\varepsilon \kappa^2 \psi \tag{10}$$

The source term due to the electric field is computed analytically using Eqs. (8) to (10), and the Navier-Stokes equations are solved numerically using the finite volume method.

Eq. (2) can be written as follows:

$$\rho_f (\mathbf{u} \cdot \nabla)\mathbf{u} = -\nabla p + \mu_f \nabla^2 \mathbf{u} + \varepsilon \kappa^2 \psi \nabla \phi \tag{11}$$

The temperature field can be obtained using the following energy equations:

$$\mathbf{u}\cdot\nabla(\rho_f c_{p,f} T_f) = \nabla\cdot(k_f \nabla T_f)\,, \quad \text{(for the fluid)} \tag{12}$$

and $$\nabla\cdot(k_s \nabla T_s) = 0\,, \quad \text{(for the substrate conduction)} \tag{13}$$

The formulated numerical model is set to solve for three-dimensional pressure-driven, electroosmotic, and mixed flows and conjugate heat transfer with the help of a commercial multiphysics solver CFD ACE+ [18].

The silicon parts of the microchannel heat sink at the inlet and outlet are set, as adiabatic boundaries and symmetric boundaries are applied at the two extreme planes in the *z*-direction. A no-slip condition is applied at the interior walls of the microchannel with thermal interface. The thermal boundary conditions in the y-direction are

$$-k_s \frac{\partial T_s}{\partial y} = q \quad \text{at } y = -(L_y - H_c).$$

$$k_s \frac{\partial T_s}{\partial y} = 0 \quad \text{at } y = H_c$$

Pressure boundary conditions are applied for the PDFs; an electric potential is applied for EOFs; and both pressure and electric potentials are assigned for mixed pressure-driven and EOFs. The overall thermal resistance of a microchannel is defined as:

$$R_{th,over} = R_{th,cond} + R_{th,conv} + R_{th,cal} = \frac{\Delta T_{max}}{qA_s} \tag{14}$$

where A_s is the area of the substrate subjected to heat flux. ΔT_{max} is the maximum temperature rise in the heat sink and is defined as:

$$\Delta T_{max} = T_{s,o} - T_{f,i} \tag{15}$$

where $T_{s,o}$ is the substrate temperature near the outlet, and $T_{f,i}$ is the fluid inlet temperature.

3. Results and discussion

The code uses a finite volume solver for both PDFs and EOFs, which applies the SIMPLEC algorithm [19] for pressure correction. The grid independence is checked, and a 175×21×71 structural grid is used for both EOFs and PDFs. The electrokinetic and thermodynamic properties of the fluid (deionized ultrafiltered water at a concentration of 10^{-6} M) are assumed to be constant and independent of the temperature to reduce computational load, which can be justified by a low velocity and a small temperature change. The numerical scheme is validated for both PDFs and EOFs for a smooth microchannel. For PDFs, the numerical scheme is validated by the results obtained by Tuckerman and Pease [1] as shown in Table 1. The numerical predictions show quite appreciable agreements with the experimental results under the same flow conditions. For the validation of the EOF scheme, the analytical solutions of Arulanandam and Li [10] are reproduced, as shown in Fig. 3, along with the numerical results obtained by Morini et al. [13]. These numerical validations provide reasonable ground for the simulation of pressure-driven and electroosmotic convective flows. The two solution schemes are coupled in the CFD ACE+, as explained in the mathematical formulation, to solve the mixed pressure-driven and electroosmotic flows. The solutions are then made to converge to a residual value of 10^{-6} for electric potential, velocity, pressure, and temperature.

The microchannel has been analyzed in terms of overall thermal resistance ($R_{th,over}$), which is indicative of the heat transfer performance of the microchannel heat sink [20] for the pressure drop and applied electric field. For a fully developed PDF, the conductive thermal resistance ($t/(k_s L_x L_y)$) and convective thermal resistance ($1/hA_{fs}$) are constant [21]. An increase in the flow rate leads to a decrease in caloric thermal resistance ($1/\dot{m}c_{p_f}$), which consequently decreases the overall thermal resistance. To determine the characteristic behavior of a microchannel heat sink driven by a mixed source of pressure and electric potential, the flow rate and thermal resistance are studied. Qualitatively, the flow rate and thermal resistance show the same behavior in both PDFs and EOFs as shown in Fig. 4. The gradient of thermal resistance with source value changes significantly in both EOFs and PDFs, which opens the doors for the proper selection of the driving source for a particular geometry under consideration. The microchannel is studied in detail with a mixed source of electric potential (15 kV) and pressure drop (10 kPa).

A microchannel heat sink is investigated for the change in zeta potential as shown in Fig. 5. The values of the zeta potential is set at 0.1 V, 0.15 V, and 0.2 V at a concentration of 10^{-4} M, 10^{-5} M, and 10^{-6} M, respectively, in view of the experimental results [8]. Flow velocity is directly related to the Helmholtz-

Table 1. Comparison of numerically predicted thermal resistances with the experimental results by Tuckerman and Pease [1] for a pressure-driven microchannel heat sink.

	Case 1	Case 2	Case 3
W_c (μm)	56	55	50
W_w (μm)	44	45	50
H_c (μm)	320	287	302
H (μm)	533	430	458
q (W/cm^2)	181	277	790
R_{th} (K/W) Exp.	0.110	0.113	0.090
R_{th} (K/W) Present cal.	0.113	0.112	0.091

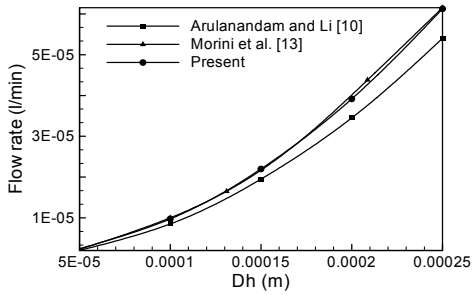

Fig. 3. Comparison of the present numerical scheme with the analytical and numerical solutions for pure electroosmotic flow.

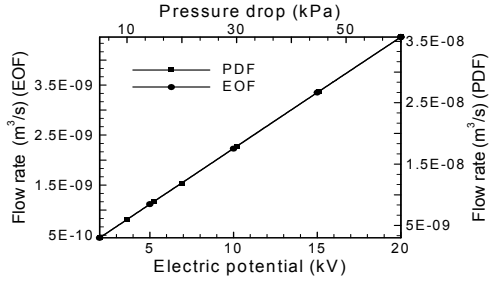

(a)

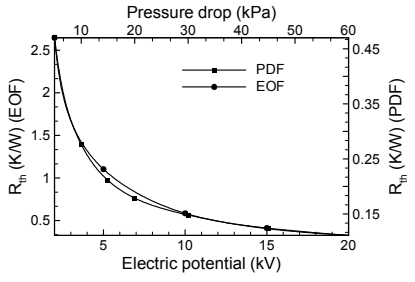

(b)

Fig. 4. Changes in the flow rate and thermal resistance, with a pressure drop and electric potential for pressure-driven flow (PDF) and electroosmotic flow (EOF): (a) flow rate and (b) thermal resistance.

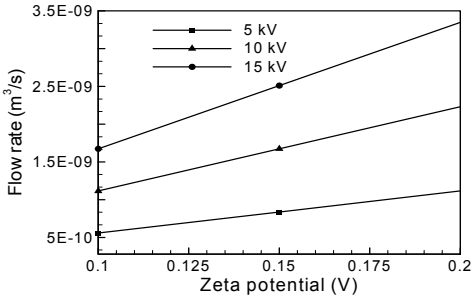

(a)

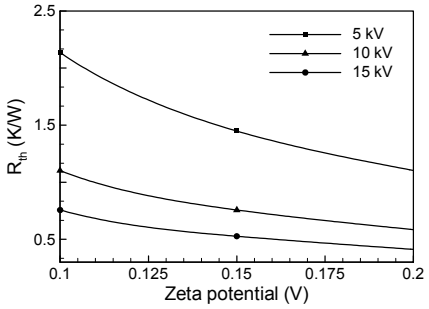

(b)

Fig. 5. Effects of the zeta potential on (a) Flow rate and (b) Thermal resistance.

Smoluchowski velocity [22] for constant cross-sectional duct; hence, it changes linearly with the zeta potential in the absence of any pressure gradient. The rate of change of the flow rate with the zeta potential increases with the increase in the applied external electric potential. Thermal resistance is affected by the applied flow conditions, hence influenced by the zeta potential or external electric potential. With the increase of the zeta potential, the Helmholtz-Smoluchowski velocity increases; hence, the flow rate increases and the thermal resistance decreases in the microchannel as evident in Fig. 5. Moreover, the rate of increase of the flow rate and the rate of decrease of the thermal resistance with the zeta potential change significantly over the varying electric potentials in the range 5 kV to 15 kV.

The flow rate and thermal resistance are further studied for mixed flow (PDF+EOF) over a wide range of source pressure drops and electric potentials. The velocity profiles on a channel cross-section are shown in Fig. 6(a) and (b) for EOF, PDF, and mixed flows in the y- and z-directions at $x/L_x = 0.5$, $z/W_c = 0.5$, and $x/L_x = 0.5$, $y/H_c = 0.5$, respectively. The merger of the plug-like velocity profile induced from the

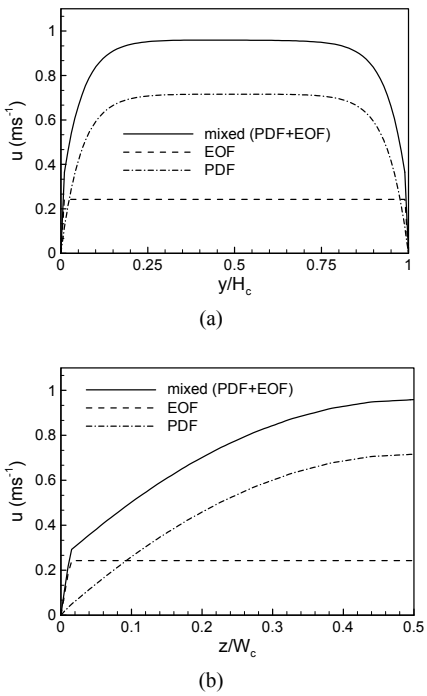

Fig. 6. Distributions of velocity in the (a) y-direction at x/L_x = 0.5, z/W_c = 0.5, and the (b) z-direction at x/L_x = 0.5, y/H_c = 0.5 for pressure-driven flow (PDF), electroosmotic flow (EOF), and mixed flow (PDF+EOF).

EOF into the PDF resulted in a reduced thermal boundary layer. The temperature profiles in various directions are shown in Fig. 7 for EOF, PDF, and mixed flow. The fully developed flow thermal characteristics are obtained for pure EOF, whereas the thermal entry length increases with the application of pressure as shown in Fig. 7(a). The surface to bulk fluid temperature difference is smallest in the EOF and highest in the PDF; therefore, higher heat transfer is obtained for mixed flows compared with the PDF. The effect of the electric field on flow rate and thermal resistance does not change significantly with the change of pressure in the mixed driving source as shown in Fig. 8. The equivalent pressure head developed by the mixed flow is shown in the Fig. 9, which represents the pressure drop in the pressure-driven microchannel at the same flow rate as obtained in the mixed flow simulations. Equivalent pressure head increases linearly with the applied pressure drop at a fixed external electric potential of 10 kV, but a higher increase is obtained at a higher applied pressure drop. The effects of the electrical potential are more pronounced at low pressure-based mixed flows where the

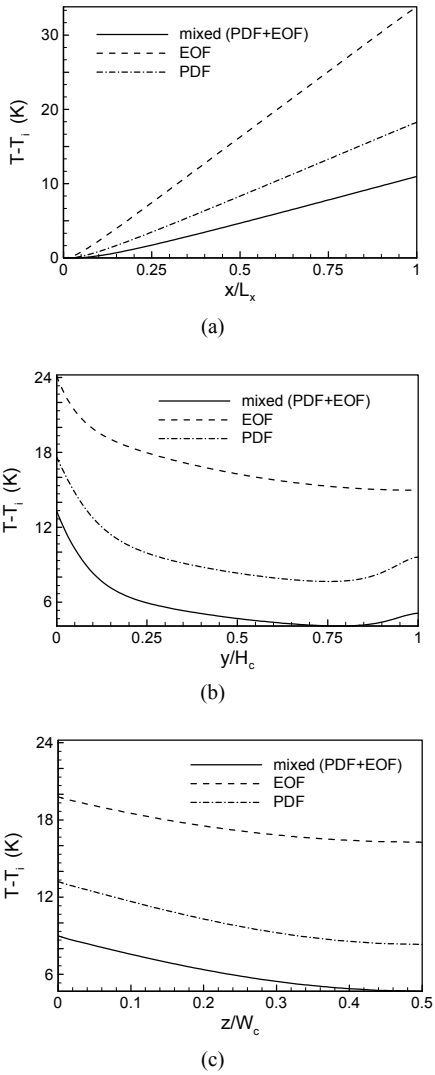

Fig. 7. Temperature profiles in the (a) x-direction at y/H_c = 0.5, z/W_c = 0.5, (b) y-direction at x/L_x = 0.5, z/W_c = 0.5, and (c) z-direction at x/L_x = 0.5, y/H_c = 0.5 for pressure-driven flow (PDF), electroosmotic flow (EOF), and mixed flow (PDF+EOF).

equivalent pressure head developed by the EOF is comparable to the applied pressure.

4. Conclusions

Current state-of-the-art micropumps used in various applications do not seem to satisfy the demand for pumping power required in micro devices, especially in electronic cooling applications. The alternative viable option is to utilize electrokinetics to assist

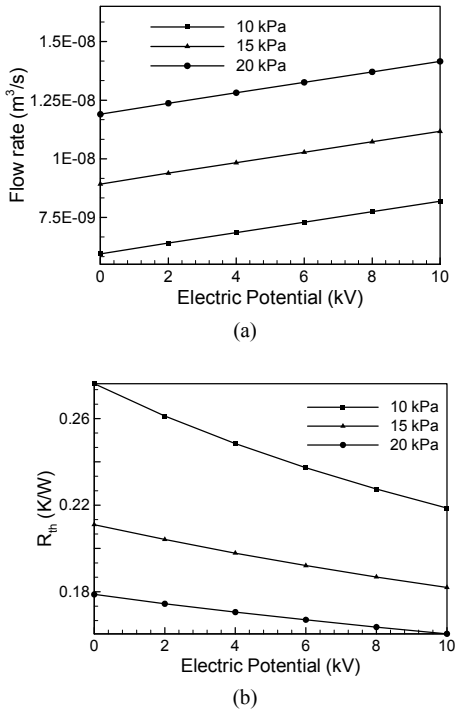

Fig. 8. Effects of the electric potential on (a) Flow rate and (b) Thermal resistance in mixed flow (EOF+PDF).

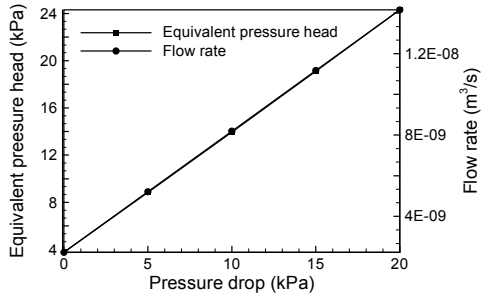

Fig. 9. Equivalent pressure head and flow rate at the electric potential of 10 kV and pressure drop ranging from 0 kPa to 20 kPa for mixed electroosmotic and pressure-driven flows.

the existing driving mechanisms. A microchannel heat sink used in electronic cooling is investigated and characterized for the suitability of its application under mixed EOFs and PDFs. The bulk fluid driving-force given by the electroosmosis phenomenon is utilized to drive the fluid into the microchannels of the heat sink. The equivalent pressure head build up by electroosmosis can be effectively used to reduce the pumping load and consequently the temperature of the microprocessor within the limited space provided. Further analysis is required to investigate a more robust model that allows the properties of the coolant to vary with the temperature and takes into account the Joule heating effects, which could be significant at high external electric field applications and high flow rates.

Acknowledgement

This work was supported by INHA UNIVERSITY Research Grant.

Nomenclature

A_s	:	Surface area of substrate base
A_{sf}	:	Area of solid and fluid interface
Dh	:	Hydraulic diameter
c_p	:	Specific heat
E	:	Electric field
H_c	:	Microchannel depth
h	:	Heat transfer coefficient
k	:	Thermal conductivity
L_x, L_y, L_z	:	Length, height, and width of the heat sink, respectively
$\dot{m}$	:	Mass flow rate
p	:	Pressure
q	:	Heat flux
R_{th}	:	Thermal resistance
t	:	Thickness of the base
T	:	Temperature
$\boldsymbol{u}$	:	Liquid velocity
W_c	:	Width of the microchannel
W_w	:	Fin width
x, y, z	:	Orthogonal coordinates

Greek symbols

ε	:	Permittivity of fluid
Φ	:	Electric potential
ϕ	:	Electric potential due to external electric field
κ	:	Debye-Hückel parameter
μ	:	Dynamic viscosity
ρ	:	Density
ρ_e	:	Electric charge density
ψ	:	Electric potential due to charge distribution within the Debye layer

Subscripts

cal	:	Caloric value
cond	:	Conductive value

conv	:	Convective value
f, s	:	Fluid and substrate, respectively
i, o	:	Inlet and outlet, respectively
max	:	Maximum value
over	:	Overall value

References

[1] D. B. Tuckerman and R. F. W. Pease, High-performance heat sinking for VLSI, *IEEE Electron device Lett.*, EDL-2 (5) (1981) 126-129.

[2] Y. Yener, S. Kakac, M. Avelino and T. Okutucu, Single-phase forced convection in microchannels: A State-of-the-Art Review, In: S. Kakac, L. L. Vasiliev, Y. Bayazitoglu, and Y. Yener (ed), *Micro-scale Heat Transfer*, Springer, Neatherlands, 2005.

[3] W. Qu and I. Mudawar, Analysis of three dimensional heat transfer in micro-channel heat sinks, *International Journal of Heat and Mass Transfer*, 45 (19) (2002) 3973-3985.

[4] K. C. Toh, X. Y. Chen and J. C. Chai, Numerical computation of fluid flow and heat transfer in microchannels, *International Journal of Heat and Mass Transfer*, 45 (2002) 5133-5141.

[5] Z. Li, X. Huai, Y. Tao and H. Chen, Effects of thermal property variations on the liquid flow and heat transfer in microchannel heat sinks, *Applied Thermal Engineering*, 27 (2007) 2803-2814.

[6] Y. Joshi and X. Wei, Micro and meso scale compact heat exchangers in electronics thermal management-A review, In: R. K. Shah, M. Ishizuka, T. M. Rudy, and V. V. Wadekar (ed), *Proceedings of fifth international conference on Enhanced, Compact and Ultra-Compact Heat Exchangers: Science, Engineering and Technology*, Engineering Conferences International, Hoboken, NJ, USA, (2005).

[7] D. J. Laser and J. G. Santiago, A review of micropumps, *Journal of Micromechanics and Microengineering*, 14 (2004) R35-R64.

[8] G. M. Mala, D. Li, C. Werner, H.-J. Jacobasch and Y. B. Ning, Flow characteristics of water through a microchannel between two parallel plates with electrokinetic effects, *International Journal of Heat and Fluid Flow*, 18 (1997) 489-496.

[9] C. Yang, D. Li and J. H. Masliyah, Modeling forced liquid convection in rectangular microchannels with electrokinetic effects, *International Journal of Heat and Mass Transfer*, 41 (1998) 4229-4249.

[10] S. Arulanandam and D. Li, Liquid transport in rectangular microchannels by electroosmotic pumping, *Coll Surf-A: Physicochemical Engineering Aspects*, 161 (2000) 89-102.

[11] L. Jiang, J. Mikkelsen, J.-M. Koo, D. Huber, S. Yao, L. Zhang, P. Zhou, J. G. Maveety, R. Prasher, J. G. Santiago, T. W. Kenny and K. E. Goodson, Closed-Loop electroosmotic microchannel cooling system for VLSI circuits, *IEEE Transactions on Components and Packaging Technologies*, 25 (3) (2002) 347-355.

[12] N. A. Patankar and H. H. Hu, Numerical simulation of electroosmotic flow, *Anal. Chem*, 70 (1998) 1870-1881.

[13] G. L. Morini, M. Lorenzini, S. Salvigni and M. Spiga, Thermal performance of silicon micro heat-sinks with electrokinetically-driven flows, *International Journal of Thermal Science*, 45 (2006) 955-961.

[14] P. Dutta, K. Horiuchi and H.-M. Yin, Thermal characteristics of mixed electroosmotic and pressure-driven microflows, *Comp. Math. Appli.*, 52 (2006) 651-670.

[15] A. Jain and M. K. Jensen, Analytical modeling of electrokinetic effects on flow and heat transfer in microchannels, *International Journal of Heat and Mass Transfer*, 50 (2007) 5161-5167.

[16] G. Tang, D. Yan, C. Yang, H. Gong, C. Chai and Y. Lam, Joule heating and its effects on electrokinetic transport of solutes in rectangular microchannels, *Sensors and Actuators A*, 139 (2007) 221-232.

[17] A. J. Bard and L. R. Faulkner, *Electrochemical methods: Fundamentals and applications*, Wiley, New York, USA, (1980).

[18] CFD-ACE+, *Software manuals*, CFD Research Corporation, (2007).

[19] J. P. Van Doormaal and G. D. Raithby, Enhancements of the SIMPLE method for predicting incompressible fluid flows, *Numerical Heat Transfer*, 7 (1984) 147-163.

[20] D. Liu and S. V. Garimella, Analysis and optimization of the thermal performance of microchannel heat sinks, *International Journal for numerical methods in Heat and Fluid flow*, 15 (1) (2005) 7-26.

[21] F. P. Incropera and D. P. DeWitt, *Fundamentals of heat and mass transfer*, John Wiley & Sons Inc, New York, USA, (2002).

[22] R. F. Probstein, *Physicochemical hydrodynamics*, Wiley and Sons Inc, New York. USA, (1994).

Afzal Husain received B.E. and M.Tech. degrees in Mechanical Engineering with specialization in Thermal Sciences from Aligarh Muslim University, India in 2003 and 2005, respectively. Currently he is pursuing Ph.D. degree in Thermodynamics and Fluid Mechanics in Inha University, Republic of Korea. His research interests are numerical analysis and optimization of heat transfer systems using computational fluid dynamics and surrogate models, development of heat transfer augmentation techniques for conventional and micro systems, thermal analysis of microelectromechanical systems (MEMS), and electronic cooling.

Kwang-Yong Kim received a B.S. degree from Seoul National University in 1978, and his M.S. and Ph.D. degrees from Korea Advanced Institute of Science and Technology (KAIST), Korea, in 1981 and 1987, respectively. Presently, he is professor and chairman, School of Mechanical Engineering, Inha University, Incheon, Korea. Prof. Kim is presently the editor-in-chief of Transactions of Korean Society of Mechanical Engineers (KSME), the editor-in-chief of International Journal of Fluid Machinery and Systems (IJFMS), and chief vice president of Korean Fluid Machinery Association (KFMA). Prof. Kim is Fellow of American Society of Mechanical Engineers (ASME).